International Journal of Zoology and Applied Biosciences **ISSN: 2455-9571**
Volume 11, Issue 1, pp: 239-247, 2026
https://doi.org/10.55126/ijzab.2026.v11.i01.031 **http://www.ijzab.com**

Research Article

PREPARATION AND CHARACTERIZATION STUDIES OF STRUCTURAL, FUNCTIONAL, MORPHOLOGICAL AND MEDICAL TREATMENT IN ANTIMICROBIAL ACTIVITY OF TIN OXIDE NANO PARTICLES

***[1]Sappani Muthu M, [2]Arul Ravi S, [3]Sathyananth M, [4]Ajith P, [4] Prem Anand D**

[1]Department of Electronics, St. Joseph's college (Autonomous) Tirchirappalli – 620 002 Tamil Nadu, India
[2]Department of Mathematics, St. Xavier's College (Autonomous), Palayamkottai- 627002, Tamil Nadu, India
[3]Department of Botany (PMRU); Zoology (CARE), St. Xavier's College (Autonomous), Palayamkottai- 627002, Tamil Nadu, India
[4]Department of Physics, St. Xavier's College (Autonomous), Palayamkottai- 627002, Tamil Nadu, India

Article History: Received 27th October 2025; Accepted 17th December 2025; Published 1st January 2026

ABSTRACT

Tin oxide nanoparticles (SnO_2 NPs) are emerging as promising antibacterial agents that work against both gram-negative and gram-positive bacteria. In this study, SnO_2 NPs were successfully synthesized using the hydrothermal method. The synthesized SnO_2 nanoparticles were analyzed using various techniques, including X-ray diffraction (XRD), Fourier-transform infrared spectroscopy (FTIR), scanning electron microscopy (SEM), and Raman spectroscopy. The cytotoxicity of the synthesized SnO_2 nanoparticles was evaluated, and their antibacterial properties were tested against Gram-negative E. coli and Gram-positive S. aureus using the disc diffusion method. The results demonstrated significant antibacterial activity of SnO_2 nanoparticles, highlighting their potential for various biomedical applications.

Keywords: Nano particles, XRD, FTIR, SEM, Raman, Hydrothermal method, Tin oxide.

INTRODUCTION

Nanotechnology has emerged as a transformative force in the field of healthcare, and also demonstrating significant potential for advancement in recent decades (Muthu *et al* 2023). It has revolutionized surgical techniques (Guan *et al.,* 2020; Muthu *et al.,* 2022) and promise in developing nano-based therapeutic solutions. International research collaborations have driven substantial growth in nanotechnology for medical devices, which enabling effective disease management globally (Pourmadadi *et al.,* 2024). However, the market for nanotechnology-based medical devices faces challenges such as high costs and stringent regulatory processes that delay product validation. Nevertheless, scientists are leveraging nanotechnology to innovate smart drug delivery systems aim at enhancing efficacy (Muthu *et al.,* 2022). Scientists have pioneered novel techniques for fabricating metal nanoparticles adorned with various functional groups to precisely target specific areas of the body, such as cancerous tumors (Ifijen *et al*. 2023). These nanoparticles, ranging in size from 1 nm to 100 nm, can be coated with a diverse array of functional groups, making them promising candidates for treating various types of cancers (Kumar *et al* 2023). By encapsulating drugs that are otherwise insoluble or face challenges in reaching their targets through conventional means; these small-sized nanoparticles effectively overcome biological barriers such as membranes (Kumar *et al* 2023), skin and the colon. Coating nanoparticles with different functional groups, such as proteins, enhance their therapeutic potential (Muthu *et al* 2023). This innovative approach enables pharmacists to devise strategies for precisely orienting proteins on the surface of metal nanoparticles (Simeonidis *et al*. 2023). This method ensures the integrity of the proteins, enhances the efficacy of the drugs, and facilitates the expansion of nanodrug applications (Uday *et al*., 2023). There is potential to establish a universal method for attaching proteins to nanoparticles that could be widely applicable across various proteins. Such a method would be of significant interest to pharmaceutical companies, particularly in the realms of

*Corresponding Author: Sappani Muthu M, Department of Electronics, St. Joseph's college (Autonomous) Tirchirappalli-620 002 Tamil Nadu, India Email: sappanimuthu_el2@mail.sjctni.edu

biosensors, drug delivery, and cognitive kits incorporating nanomaterials (Humphrises *et al.,* 2021). Therefore, prior investigation into the protein-nanoparticle interaction is crucial for developing effective nano-based antiproliferative drugs. The properties of tin oxide (SnO_2) nanoparticles include chemical stability, thermal stability, and biocompatibility. SnO_2 nanoparticles have demonstrated significant potential in applications such as sensor development and drug delivery systems. Their unique geometry and structural properties allow for efficient drug loading and controlled release at specific target sites. Additionally, the surface of SnO_2 nanoparticles can be functionalized with various chemical groups, enabling them to bind effectively with a wide range of therapeutic molecules (Pandey *et al*., 2021). These nanoparticles are widely utilized in numerous biomedical fields, including diagnostics, targeted drug delivery, cancer therapy, imaging, bioassays, and cellular uptake. For effective cancer treatment, candidates must be capable of circulating through the bloodstream and reaching designated target sites. Biomolecules like human serum albumin (HSA), the most abundant protein in human blood plasma, play a critical role in this process. HSA's abundance in the circulatory system and its exceptional binding capacity for a wide array of molecules make it invaluable for studying the pharmaco dynamics and pharmacokinetics of anti proliferative drugs. Accordingly, the purpose of this study was to investigate the synthesis of SnO_2 by hydrothermal methods, investigate their interactions with HSA, and evaluate their anti proliferative effects on human leukemia K562 cells by using both experimental and computational methodologies.

MATERIALS AND METHODS

Preparation of Tin oxide

In order to synthesize SnO_2 nanoparticles, a solution of 0.03 M stannous chloride dihydrate ($SnCl_2 \cdot 2H_2O$, AR grade) was prepared. Adding 5 ml of ammonia solution to this solution gradually turned the pH from 7 to 10 when the ammonia solution was added. A magnetic stirrer was then used to stir the mixture at 80°C for 30 minutes using a magnetic stirrer. The solution was then sealed, placed in a microwave oven, and heated without an exhaust fan for six minutes at 800 Watts, reducing the volume to one fourth of what it had been before it was heated in the microwave. The results of this process were then filtered by using filter paper in order to remove impurities from the colloidal solution. After filtering the solution, it was washed 2-3 times with deionized water to further improve the purity of the solution. A third step was to allow the wet nanoparticles to air dry for three days after they were stirred this synthesis process shown in Figure 1.

Figure 1. Synthesis Process of Tin Oxide.

Characterization

The crystal structure was examined unden X-ray diffraction (XRD) using an X-ray diffractometer (Rigaku TTRIII, Rigaku Corporation, Japan) with Cu Kα radiation (1.54056 Å). Additionally, field-emission scanning electron microscopy (FESEM) was conducted with an FEI QUANTA 200 instrument (FEI Company, USA).

Antibacterial activity

Tin oxide (SnO_2) nanoparticles were suspended in 40% dimethyl sulfoxide (DMSO) to create test solutions at various concentrations. Antimicrobial efficacy was assessed from (Humphries *et al* 2021). Sterile filter paper discs (6 mm diameter) were impregnated with 20 µL of SnO_2 nanoparticle suspensions and dried aseptically. The antibacterial activity was tested against five clinically relevant human pathogens, including both Gram-positive and Gram-negative bacteria. The pathogens included Staphylococcus aureus (MTCC 96), Escherichia coli (MTCC 443), Klebsiella pneumoniae (MTCC 3384), Bacillus subtilis (MTCC 441), and Salmonella typhimurium (MTCC 98). Mueller-Hinton agar plates were inoculated with standardized bacterial suspensions (0.5 McFarland standard). Impregnated discs were placed on the agar surface, and the plates were incubated at 37°C for 18-24 hours. Zones of inhibition were measured to the nearest millimeter using digital calipers.

The percentage of inhibition for each pathogen was calculated using:

$$\mathbf{PI} = \frac{\mathbf{100\ x\ (X - Y)}}{\mathbf{(Z\ -\ Y)}}$$

X = Mean test extract,

Y = Mean negative control,

Z = Mean positive control.

Statistical analysis was performed using one-way ANOVA followed by Tukey's post-hoc test ($p < 0.05$). Experiments were conducted in triplicate, with results expressed as mean ± standard deviation (SD).

RESULT AND DISCUSSION

The X-ray diffraction (XRD) pattern of SnO_2 nanoparticles synthesized by using the hydrothermal method that is provided below. All peaks correspond to the tetragonal structure of tin oxide (JCPDS 41-1445). The main peak occurs at $2\theta = 26.53°$ with a peak width of 0.933 nm. Using the Debye-Scherrer formula, the average crystallite size (D) of the nanoparticles is estimated to be approximately 47.35 nm, indicating a tetrahedral shape. The average dislocation density of the SnO_2 particles is determined to be $7.28\times10^{14}/m^2$ using an appropriate equation. Figure 2. Shows the XRD pattern of SnO_2 nanoparticles. The diffraction peaks, originating from the (110), (101), and (211) planes, are located at a 2θ of 26.52°, respectively. Diffraction peaks match well with JCPDS file 41-1445 from the Joint Committee for Powder Diffraction Standards. SnO_2 nanoparticles after thermal treatment are pure and crystalline, with no impurities visible. SnO_2 nanopowder that has been prepared as-prepared exhibited diffraction peaks that are similar to those found in bulk SnO_2, indexed to the orthorhombic crystal structure. The calculated lattice parameters for this crystal structure as selected by JCPDS are a =0.429 nm, b = 1.191 nm, and c = 0.388 nm. A sharper and broader peak is evident on the graph, and the size of the crystallites has been reduced also, confirming the reduction in size. By use of the Scherrer formula, we were able to determine the average diameter of the crystallite to be around 26.53 nm.

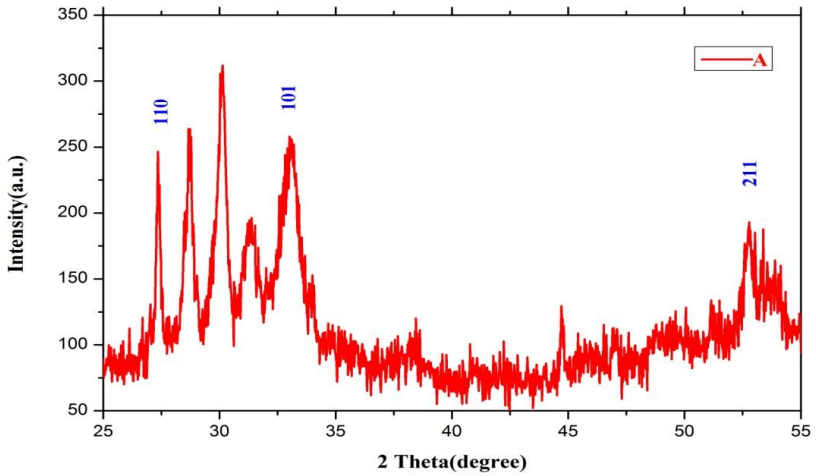

Figure 2. XRD spectrum for SnO_2 nanoparticle.

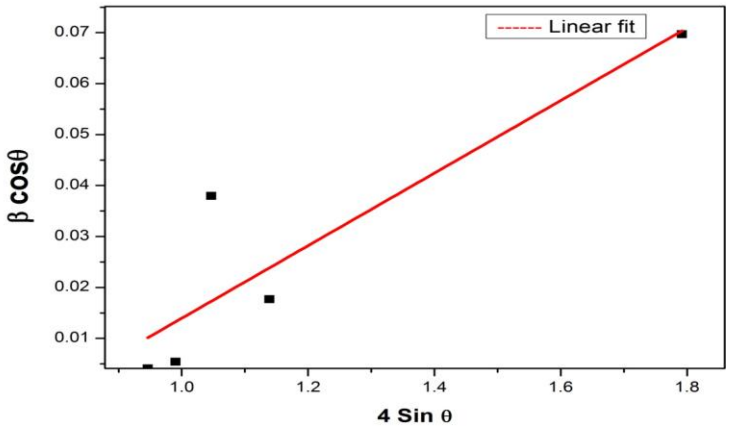

Figure 3. W- H Plot.

The William son - Hall (W-H) plot method is used to calculate the crystal size and strain of the Hydrothermal synthesized SnO_2 nano Particle from XRD data using the William son - Hall (W-H) plot method. Due to the incoherent diffraction domains, micro strains are induced in the SnO_2 nano particle to their incoherence. The experimental data of the XRD pattern show that the peak width is both broadening and the peak terms are interrelated by the equation, where the peak size (time, spot, and factor) and the peak width (T) are related by the equation, indicating the smaller crystal size of the nanoparticles. A total broadening can be calculated by dividing the crystallite size by the strain (crystallite size + strain). As can be seen in the Equation, it indicates a linear equation in which the slope of the linear fit is used to calibrate crystalline size, while the Y - intercept is used to calculate the crystal size from the slope of the linear fit. It can be studied using the W-H plot by plotting the graph between the 4 sin θ coordinates of the nanocrystalline size and the Y coordinate of the micro strain. According to the graph shown in Figure 3, the value of micro strain is 7.121 x 10^{-4} and the crystal size is 28.14 nm.

SEM is a type of microscope that uses electron beams to identify samples to produce images of the samples that are being examined. A sample's surface is affected by these electrons, which interact with the surface of the sample, revealing details about its composition and topography. To examine the surface morphology of SnO_2 nanoparticles, SEM analysis has been used to conduct an analysis using SEM techniques. SEM images of the nanoparticles at various magnifications (10 µm, 3 µm, 2 µm, 1 µm) are shown in Figure 4. (a) and 4. (b). The images reveal that the particles have an irregular morphology with different sizes and are highly agglomerated. Figure 4. (c, d) shows the spherical structure of tin oxide, displaying a homogeneous microstructure in all samples. The presence of agglomerates was not detected, but the sample exhibited a highly porous microstructure. The EDAX spectra of the synthesized nanoparticles are depicted in Figure 5. The micrographs verify that, consistent with the findings of (Gadkari *et al*. 2020), SiO_2 nanoparticles are evenly applied on the surfaces of cotton fabric. The EDAX spectra reveal the presence of peaks associated with the elements tin (Sn) and oxygen (O).

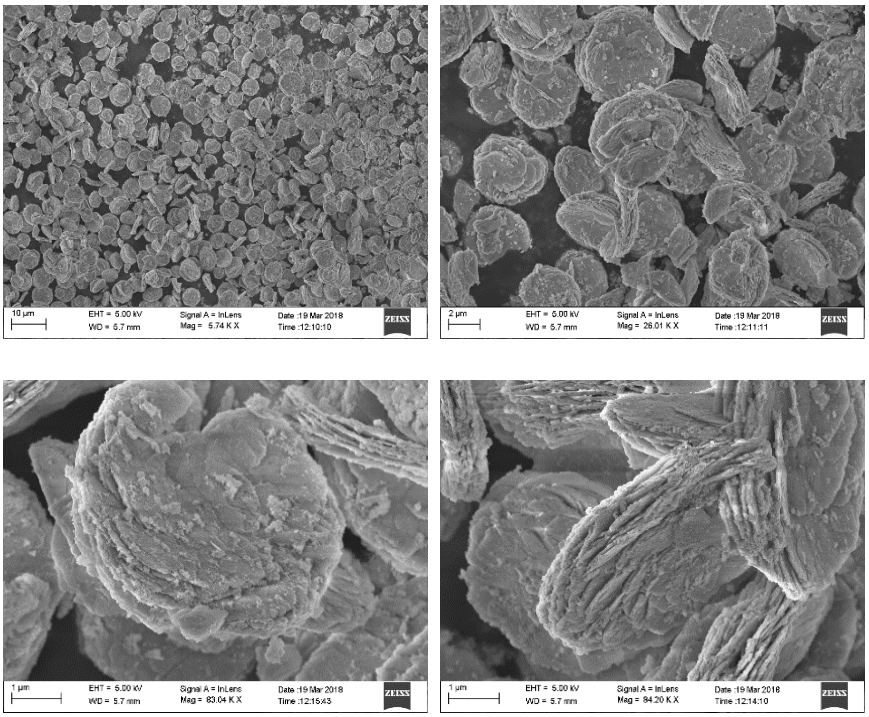

Figure 4. (a, b, c, d) SEM images of Tin oxide.

Table 1. EDAX spectrum of tin oxide.

Element	Weight%	Atomic%
O K	21.34	49.23
Cl K	2.29	4.39
Sn L	78.65	46.38
Totals	102.29	100

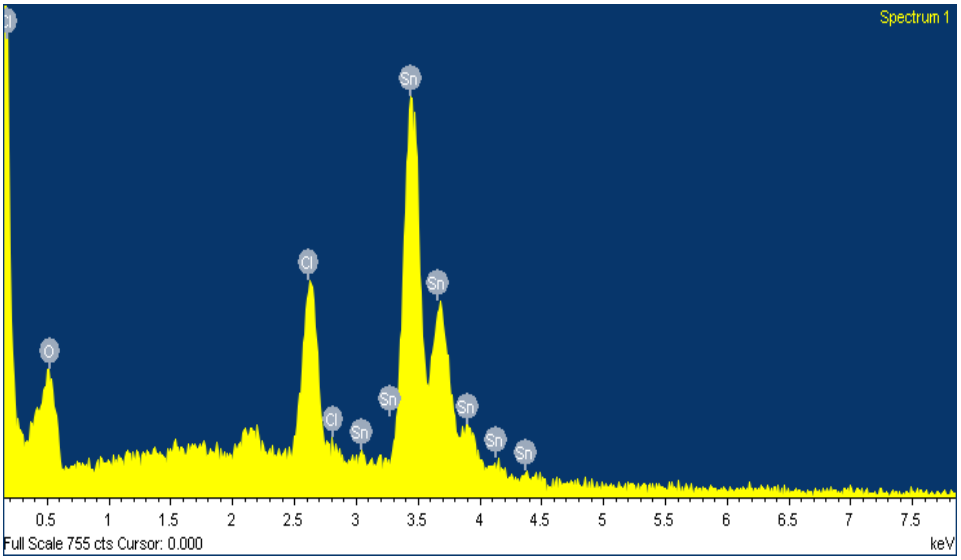

Figure 5. EDAX spectra of tin oxide.

Figure 6 shown in the functional groups present in SnO_2 nanomaterials were analyzed using FTIR, with the study conducted over a range of 400 cm^{-1} to 4000 cm^{-1}. In the FTIR spectroscopy graph, the band observed between 3400 and 3184 cm^{-1} indicates O-H bond stretching vibration. On SnO_2, there are OH groups and adsorbed water molecules. It corresponds to water molecules trapped in SnO_2 bending vibrations between 1618 and 1386 cm^{-1}. The peak at 564 cm^{-1} is associated with the stretching vibrations of terminal Sn-OH, while the region from 1093 to 600 cm^{-1} displays the stretching modes of Sn-O-Sn. Raman spectroscopy is frequently utilized to study nanomaterials such as SnO_2, as illustrated in Figure 7. Four distinct peaks can appear at 186 cm^{-1}, 512 cm^{-1}, 694 cm^{-1}, and 742 cm^{-1} for SnO_2, These correspond to D and G bands. sp^3 carbon molecules exhibit disordered structural defects, whereas orderly sp^2 carbon molecules exhibit G band vibrations. Lower ratios indicate a larger crystallite size, and higher ratios represent more crystallization. After electrochemically reducing SnO_2, D and G peaks increase, while their positions shift.

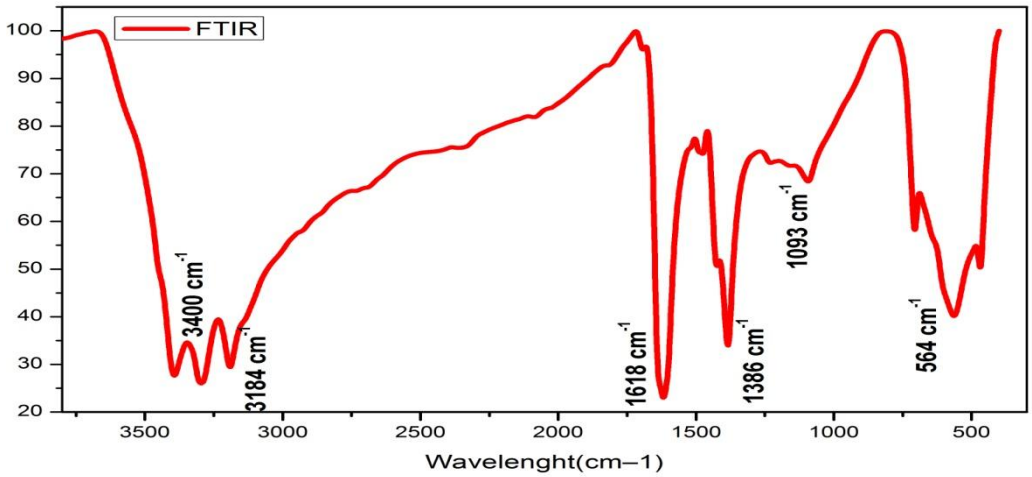

Figure 6. FTIR spectra of Tin oxide

Table 2. Raman active mode.

Modes	Frequencies (cm^{-1})
A_{1g}	694
B_{2g}	742
B_{1g}	186
E_g	512

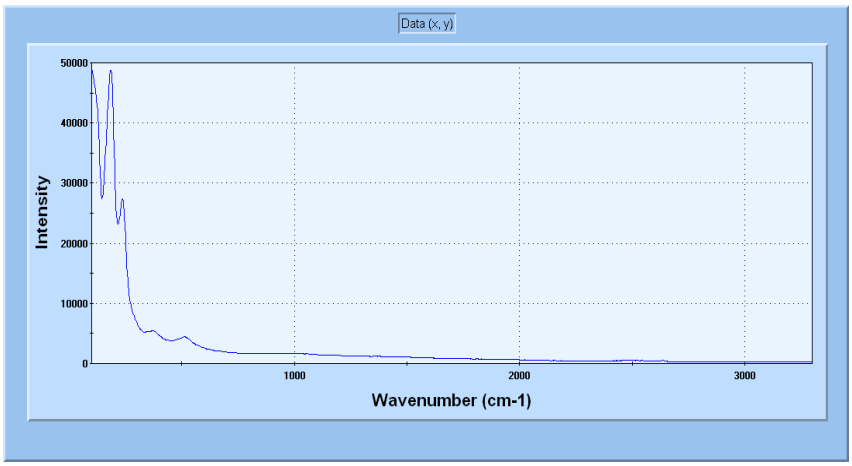

Figure 7. Raman spectra of tin oxide.

Figure 8. Shown in SnO_2 nanomaterials demonstrated varying antimicrobial activity against five pathogenic bacteria: Staphylococcus aureus, Escherichia coli, Klebsiella pneumoniae, Bacillus subtilis, and Salmonella typhimurium. The inhibitory effect increased with higher concentrations of SnO_2 nanomaterials, with the highest concentration (S3: 15 mg) showing the most significant antibacterial activity. Table 3. Inhibition percentages for S3 ranged between 55.2% and 83.8%, where E. coli being the most susceptible pathogen and S. typhimurium the least sensitive. These findings align with recent research on metal oxide nanoparticles' antimicrobial properties. Dose-dependent antibacterial activity of SnO_2 nanoparticles against various pathogens. The mechanism likely involves the generation of reactive oxygen species (ROS) and disruption of bacterial cell membranes (Guan *et al*., 2020, Sinha *et al*. (2024) demonstrated that SnO_2 nanoparticles could be an effective alternative to conventional antibiotics, especially against resistant strains. However, the streptomycin control consistently outperformed the SnO_2 nanomaterials, indicating that further optimization may be necessary for practical applications (Pandey *et al*., 2023; Khanom *et al*., 2018). Table 4. Statistical analysis (one-way ANOVA, $p < 0.001$) confirmed significant differences in antimicrobial activity across concentrations and pathogens. Post-hoc tests revealed that the highest concentration (S3) generally produced significantly larger inhibition zones compared to lower concentrations, supporting the potential of SnO_2 nanomaterials as broad-spectrum antimicrobial agents.

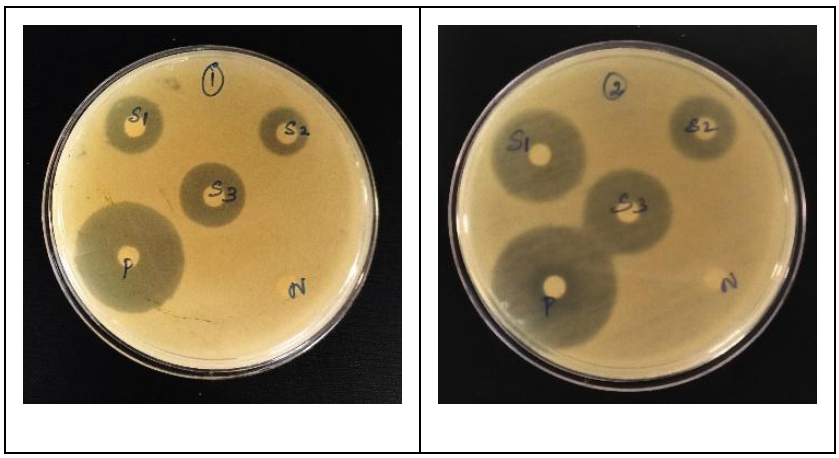

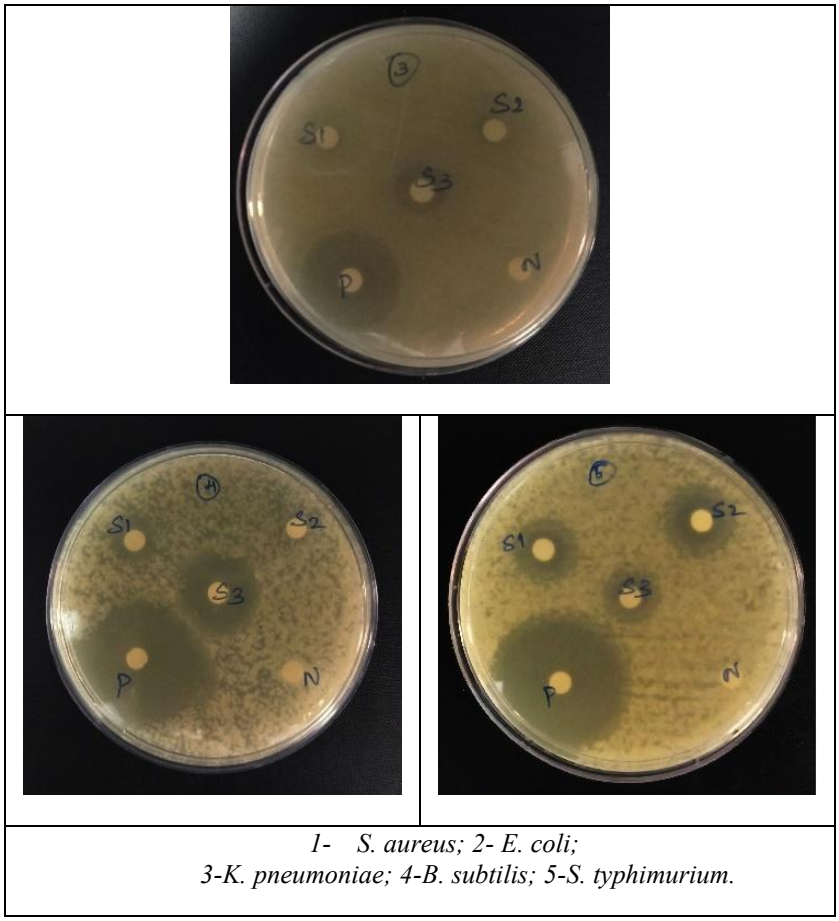

1- S. aureus; 2- E. coli;
3-K. pneumoniae; 4-B. subtilis; 5-S. typhimurium.

Figure 8. Antibacterial activity of Tin Oxide.

Table 3. Antibacterial activity inhibition.

S.No	Pathogens	Assay	ZoI (Mean ± SD)	Percentage of Inhibition
1	*Staphylococcus aureus*	S1	11.5 ± 0.5 a	56.0
		S2	12.5 ± 0.5 a	60.9
		S3	15.8 ± 0.7 b	77.0
		P	20.5 ± 0.5 c	100
2	*Escherichia coli*	S1	15.2 ± 0.5 a	64.4
		S2	18.0 ± 0.5 b	76.2
		S3	19.8 ± 0.7 b	83.8
		P	23.6 ± 1.0 c	100
3	*Klebsiella pneumoniae*	S1	8.50 ± 0.5 a	53.1
		S2	11.1 ± 1.0 a	69.3
		S3	12.6 ± 0.7 a	78.7
		P	16.0 ± 0.5 c	100
4	*Bacillus subtilis*	S1	8.83 ± 1.0 a	43.9
		S2	9.33 ± 1.0 a	46.4
		S3	15.5 ± 0.8 b	77.1
		P	20.1 ± 0.7 c	100
5	*Salmonella typhimurium*	S1	10.1 ± 1.2 a	48.0
		S2	11.8 ± 0.7 a	56.1
		S3	11.6 ± 1.0 a	55.2
		P	21.0 ± 0.5 c	100

S1- 5 mg; S2 -10 mg; S3 – 15 mg; (SnO_2 nanomaterials) Positive Control – Streptomycin (20 mcg).

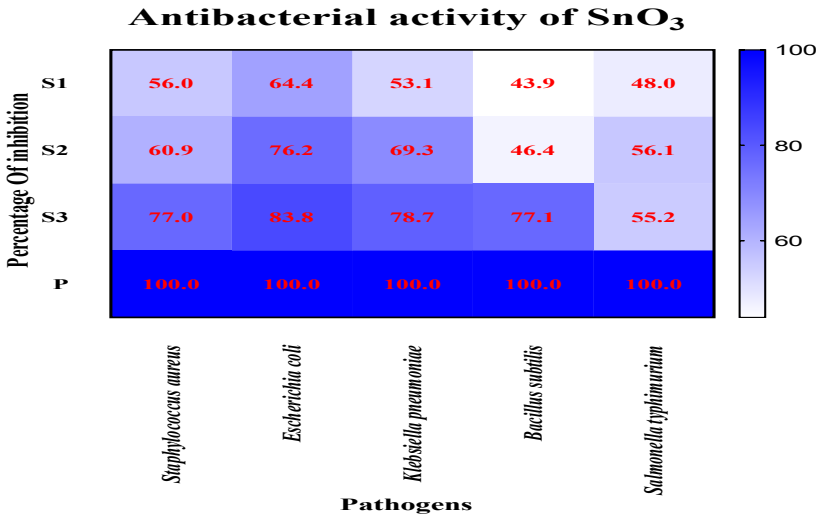

CONCLUSION

The preparation of SnO_2 nanoparticles was carried out with the aim of hydrothermal methods. The XRD patterns of both pure SnO_2 nanoparticles were in excellent agreement with the tetragonal structure of the SnO_2 and it was confirmed by that fact that they are both shaped as SnO_2 tetragonal nanoparticles. Analyzing scanning electron microscopy images of the synthesized nanoparticles is used as an analytical method for determining the surface morphology. Antibacterial activity area of inhibition *Staphylococcus aureus, E. coli, K. pneumonia, Bacillus Subtilis, Salmonella typhimurium,* these pathogenic bacteria examined highet and lowest concentration of antibacterial activity.

ACKNOWLEDGMENT

The authors would like to thank Dr. Akhila Kumar sagu, CSIR principal scientist, and Dr. Magesh kumar SPO, CSIR Chennai Tharamani Complex, Chennai, for their constant support and encouragement. The authors are very grateful for the constant support provided by Rev. Dr. Pavulraj Michael S.J, Rector, Rev. Dr. S. Mariadoss S.J, the principal of St. Joseph's college (Autonomous) Tirchirappalli, and Rev. Dr. P. Arockiasamy Xavier S.J, the secretary of St. Joseph's college (Autonomous) Tirchirappalli

CONFLICT OF INTERESTS

The authors declare no conflict of interest

ETHICS APPROVAL

Not applicable

FUNDING

This study received no specific funding from public, commercial, or not-for-profit funding agencies.

AI TOOL DECLARATION

The authors declares that no AI and related tools are used to write the scientific content of this manuscript.

DATA AVAILABILITY

Data will be available on request

REFERENCES

Muthu, M. S., Ajith, P., Agnes, J., Selvakumar, M. S., Presheth, M., & Anand, D. P. (2023). Hydrothermal synthesis and characterisation of nanographene oxide/cobalt oxide (GO/Co_3O_4) nanocomposite suitable for supercapacitor applications. *Journal of Materials Science: Materials in Electronics, 34*(25), 1766. https://doi.org/10.1007/s10854-023-11085-3.

Guan, G., Zhang, L., Zhu, J., Wu, H., Li, W., & Sun, Q. (2020). Antibacterial properties and mechanism of biopolymer-based films functionalized by CuO/ZnO nanoparticles against *Escherichia coli* and *Staphylococcus aureus*. *Journal of Hazardous Materials, 402*, 123542. https://doi.org/10.1016/j.jhazmat.2020.123542.

Muthu, M. S., Xavier, S. S. J., Ajith, P., & Anand, D. P. (2022). Preparation and characterization studies of nanographene oxide. *Materials Today: Proceedings, 66*, 2449–2454. https://doi.org/10.1016/j.matpr.2022.06.367.

Pourmadadi, M., Omrani, Z., Abbasi, R., Mirshafiei, M., & Yazdian, F. (2024). Poly (tannic acid)-based nanocomposite as a promising potential in biomedical applications. *Journal of Drug Delivery Science and Technology, 95*, 105568. https://doi.org/10.1016/j.jddst.2024.105568.

Muthu, M. S., Rejith, S. G., Ajith, P., Agnes, J., & Anand, D. P. (2022). Antibacterial activity of copper oxide nanoparticles against gram-positive and gram-negative bacterial strains synthesized by precipitation technique. *International Journal of Zoology and Applied Biosciences,* *7*(1), 17–22. https://doi.org/10.55126/ijzab.2022.v07.i01.004.

Ifijen, I. H., Ikhuoria, E. U., Omorogbe, S. O., Anegbe, B., Jonathan, E. M., & Chikaodili, D. I. (2023). Chemical, plant and microbial mediated synthesis of tin oxide nanoparticles: Antimicrobial and anticancer potency. *Brazilian Journal of Chemical Engineering, 40*(4), 965–991. https://doi.org/10.1007/s43153-023-00315-0.

Kumar, N., Tripathi, H., Kumar, S., & Bhardwaj, S. (2023). Sol–gel synthesis of tin oxide nanoparticles and their characterizations. *Materials Today: Proceedings*. https://doi.org/10.1016/j.matpr.2023.06.072.

Kumar, A., Chitkara, M., & Dhillon, G. (2023). Effect of varying calcination temperature on the structural and optical properties of tin oxide nanoparticles. *Materials Today: Proceedings*. https://doi.org/10.1016/j.matpr.2023.05.207.

Sappani Muthu, M., Ajith, P., Agnes, J., Selvakumar, M. S., Presheth, M., & Anand, D. P. (2023). Optical, thermal, and electrochemical properties of nanographene oxide/nickel oxide nanocomposite suitable for supercapacitor applications. *Materials Today: Proceedings*. https://doi.org/10.1016/j.matpr.2023.05.615.

Muthu, M. S., Ajith, P., Agnes, J., Selvakumar, M. S., Presheth, M., & Anand, D. P. (2023). Hydrothermal synthesis and characterization studies of nano graphene oxide/copper oxide (CuO) nanocomposites suitable for supercapacitor applications. *Rasayan Journal of Chemistry,* *16*(1). https://doi.org/10.31788/RJC.2023.1618190.

Simeonidis, K., Kalaitzidou, K., Asimakidou, T., Martinez-Boubeta, C., Makridis, A., Haeussler, A., … Balcells, L. (2023). Tin oxide nanoparticles via solar vapor deposition for hexavalent chromium remediation. *ACS Applied Nano Materials,* *6*(15), 13902–13911. https://doi.org/10.5281/zenodo.7589706

Uday, Y. S., Manjunatha, H. C., Vidya, Y. S., Manjunatha, S., Soundar, R., & Sridhar, K. N. (2023). Multifunctional properties of tin oxide nanoparticles synthesized by green and chemical approach. *Current Applied Physics, 55*, 9–15. https://doi.org/10.1016/j.cap.2023.08.003.

Humphries, R., Bobenchik, A., Hindler, J., & Schuetz, A. (2021). Overview of changes to the Clinical and Laboratory Standards Institute performance standards for antimicrobial susceptibility testing, M100, 31st edition. *Journal of Clinical Microbiology, 59*, e00213-21. https://doi.org/10.1128/JCM.00213-21.

Pandey, M., Singh, M., Wasnik, K., Gupta, S., Patra, S., Gupta, P., Pareek, D., Chaitanya, N., Maity, S., Reddy, A., Tilak, R., & Paik, P. (2021). Targeted and enhanced antimicrobial inhibition of mesoporous ZnO–Ag_2O/Ag, ZnO–CuO, and ZnO–SnO_2 composite nanoparticles. *ACS Omega,* *6*, 31615–31631. https://doi.org/10.1021/acsomega.1c04139.

Khanom, R., Parveen, S., & Hasan, M. (2018). Antimicrobial activity of SnO_2 nanoparticles against *Escherichia coli* and *Staphylococcus aureus* and conventional antibiotics. *American Scientific Research Journal for Engineering, Technology, and Sciences, 46*, 111–121.